



NCRA TECHNICAL REPORT

Towards Understanding the Polarization Properties of the GMRT Antennas and Electronics

Yashwant Gupta and Sanjay Kudale

NCRA-TIFR, Pune - 411 007

15 December 2001

1 Summary

We describe test observations carried out to understand some aspects of the polarization properties of the GMRT antennas and the associated electronics. The tests were carried out under different configurations of the antennas and receiver systems, while using the GMRT Phased Array receiver in the pulsar back-end as the main tool to measure the cross-correlation between two different polarization signals.

First, calibration for instrumental cross-coupling within the correlator + pulsar receiver was done using test noise sources. This calibration procedure enabled us to come up with a simple technique to test for poor isolation between the two channels of any sampler card.

The tests under conditions of (i) terminated front-end and (ii) "RF off" indicate that there is no significant cross-coupling between the two polarization chains in the IF, optical fibre and base-band sections of the electronics. Further, we find that, in these tests, the condition of MCM5 ON produces correlated noise (with specific spectral properties) between the two polarization channels, leading to the conclusion that there is a source of common pick-up (electrically coupled signal) in the two channels, somewhere in the front-end system.

Tests done with signals from the two polarizations of the same antenna (at 325 MHz) show evidence for *another* source of common noise pick-up (with relatively more uniform spectral properties) present in the front-end section. This source, which is found to have no connection with MCM5 being ON/OFF, has a typical signal strength of about $5 - 10^\circ$ K with a worst case of about 20° K. Thus, this signal normally dominates over any genuine polarization cross-coupling that may be present in the antenna and the front-end electronics.

Tests done with signals from the two polarizations (self as well as cross) of *different* antennas allow us to detect the true polarization cross-coupling at 325 MHz. The rough estimates for this are ~ 1.5 to 3% for several of the antennas, at this frequency.

Evidence for a correlated noise pick-up in the polarization channels is found at other frequency bands also. Specifically, at 610 MHz, there are strong variations of this signal across the band and it becomes quite large (\sim system noise temperature) in some parts of the band, for quite a few antennas. This could be the cause of the effective loss of sensitivity that is seen across these parts of the band for such antennas.

Our main conclusions and suggested future action are detailed at the end.

2 Introduction

The GMRT is designed to give full polarization capability at all wave-bands of observation. This means that RF signals of two orthogonal polarization states (linears for the L-band and circulars for all the other bands) are available from each antenna. These can be used for generation of all 4 Stokes parameters of the incoming radiation, for both interferometry and phased array modes of operation. As is often the problem in such cases, the orthogonality of these signals (as seen by the final back-end) is usually somewhat corrupted, mainly due to some amount of non-orthogonality in the receiving elements and some amount of leakage of signal between the two polarization paths. This effect is usually corrected by appropriate calibration of the polarization properties of the antenna plus receiver chain. This requires experiments and test observations to understand these polarization properties and to estimate the level of cross-coupling between the two orthogonal polarization signals.

Normally, polarization cross-coupling between two orthogonal polarization states received by an antenna system can be characterized (somewhat approximately) by the equations

$$V'_R = G_R (V_R + \epsilon_{RL} V_L) , \quad (1)$$

$$V'_L = G_L (V_L + \epsilon_{LR} V_R) ; \quad (2)$$

where V'_R & V'_L are the received voltage signals corresponding to the corrupted orthogonal polarization states of the incoming, true orthogonal polarization signal voltages V_R & V_L , respectively (the convention for R & L circulars is used here). We have assumed the cross-coupling parameters (ϵ_{RL} & ϵ_{LR}) to be $\ll 1$ and have therefore ignored their second order normalization terms (e.g. Gupta & Upreti, 1991; Conway & Kronberg, 1969). G_R & G_L are the effective gains for the two polarization channels. Including the effect of receiver noise, the above equations can be rewritten as

$$V'_R = G_R (V_{Rs} + \epsilon_{RL} V_{Ls} + V_{Rn}) , \quad (3)$$

$$V'_L = G_L (V_{Ls} + \epsilon_{LR} V_{Rs} + V_{Ln}) ; \quad (4)$$

where V_{Rs} & V_{Ls} refer to the signal terms (from the source) and V_{Rn} & V_{Ln} refer to the system noise terms, for the two polarizations. The above assumes that the bulk of the cross-coupling occurs *before* the LNA (e.g. in the dish, feeds and polarizer in the case of the GMRT) - we will refer to this as model 1.

A second, more complicated scenario (model 2), where part of the cross-coupling between the two polarization signal paths may also occur *after* the LNA would then look like

$$V'_R = G_R (V_{Rs} + \epsilon_{RL} V_{Ls} + V_{Rn} + \eta_{RL} V_{Ln}) , \quad (5)$$

$$V'_L = G_L (V_{Ls} + \epsilon_{LR} V_{Rs} + V_{Ln} + \eta_{LR} V_{Rn}) ; \quad (6)$$

where ϵ & η are the effective cross-coupling parameters for this distributed coupling mode. This model may be of some relevance to our study here.

It will also prove to be useful to consider yet another possibility (model 3), where the polarization cross-coupling is as in model 1, but there is a source of constant, correlated noise present in both polarization channels :

$$V'_R = G_R (V_{Rs} + \epsilon_{RL} V_{Ls} + V_{Rn} + V_c) , \quad (7)$$

$$V'_L = G_L (V_{Ls} + \epsilon_{LR} V_{Rs} + V_{Ln} + V_c) ; \quad (8)$$

Such a situation could occur in the case of the GMRT if, for example, a small part of the calibration noise power was always being coupled into the front end amplifier chain.

Normally, polarization cross-coupling parameters for a single dish are obtained from measurements of the cross and self correlations for the two voltage signals, using sources with known polarization properties.

For the current work, we will try to see what information can be obtained from such measurements, using *unpolarized* calibration sources.

A measurement of the cross-correlation between the two polarization signals yields the following (for model 1):

$$C_{RL} \equiv \langle V'_R V'^*_L \rangle = G_R * G_L^* \left(\langle V_{R_s} V_{L_s}^* \rangle + \epsilon_{LR}^* |V_{R_s}|^2 + \epsilon_{RL} |V_{L_s}|^2 \right) .$$

For an unpolarized radio source (many continuum calibration sources are weakly enough polarized to meet this criteria fairly well), the above equation reduces to

$$C_{RL} = G_R G_L^* I_s (\epsilon_{RL} + \epsilon_{LR}^*) / 2 = G_R G_L^* I_s \text{Re}[\epsilon_{RL}] ; \quad (9)$$

where I_s is the total intensity of the source and $\text{Re}[\]$ stands for the real part of the complex number. The last part in the above equation is an expression valid for a case of symmetric cross-coupling, i.e. $\epsilon_{RL} = \epsilon_{LR}$; real life situations will, in general, be much more complicated than this (especially as far as the phases of ϵ_{RL} & ϵ_{LR} are concerned). However, the above allows a quick, first-order estimate of the level of cross-coupling from simple measurements on unpolarized radio sources. A full, rigorous analysis requires extensive measurements (usually over a range of parallactic angles) of cross and self terms on polarized radio sources with well determined polarization properties (e.g. Conway & Kronberg, 1969).

From equation 10, an estimate for the cross-coupling can be obtained from sources of known strength, if the gains are known. One way to do this is to work with the normalized cross-correlation (i.e. the cross-correlation divided by the square root of the product of the self-correlations) which gives the following result (for model 1) :

$$C_{RL}^m = \frac{e^{i\phi_{RL}} I_s (\epsilon_{RL} + \epsilon_{LR}^*)}{2(I_s/2 + |V_n|^2)} = \frac{2 e^{i\phi_{RL}} T_s \text{Re}[\epsilon_{RL}]}{T_s + T_n} ; \quad (10)$$

where ϕ_{RL} is the phase difference between G_R & G_L , and T_s, T_n refer to the noise temperatures corresponding to the signal and noise powers respectively. The corresponding expression for the case of model 2 is

$$C_{RL}^m = \frac{2 e^{i\phi_{RL}} (T_s \text{Re}[\epsilon_{RL}] + T_n \text{Re}[\eta_{RL}])}{T_s + T_n} ; \quad (11)$$

and for the case of model 3 it is

$$C_{RL}^m = \frac{2 e^{i\phi_{RL}} (T_s \text{Re}[\epsilon_{RL}] + T_c)}{T_s + T_n + T_c} . \quad (12)$$

These expressions will be relevant for the analysis of the results from the cross-correlation measurements, which form the main tool of our work.

This report describes test observations carried out to understand some aspects of the polarization properties of the GMRT antennas and the associated electronics chain. The main aim was to get first order estimates of the levels of cross-coupling for a sample of antennas, at different wave-bands of operation. In the process, we have discovered some unusual polarization properties which are also reported here.

3 The Experimental Set-up

For the experiments described in this report, we used the GMRT pulsar receiver system as the main back-end to acquire the data that would give the required cross-correlation coefficients. The first part of this pulsar receiver is the GAC (GMRT Array Combiner) which has the capability to add any number of selected antenna signals (separately for each polarization) in both incoherent array mode viz., addition of intensity

signals (after square law detection) and coherent array mode viz., addition of voltage signals (before square law detection). The summing is done separately for each of the 256 spectral channels of data that is made available to the GAC from the output of the FFT stage of the GMRT correlator.

The outputs of the GAC, which are at the rate of one spectral realization every $16 \mu\text{sec.}$, are available for further processing by other pulsar back-ends. The specific back-end used in this experimental set-up is the the GPA (GMRT Phased Array) Receiver (see MSc thesis of S. Sirothia for details about this) which consists of hardware that can take the voltage signals for the two orthogonal polarizations (referred to as “pol1” and “pol2”) from the phased array output of the GAC and produce the following self and cross products between these signals :

1. Total power in pol1
2. Total power in pol2
3. Real part of the cross-correlation of pol1 and pol2.
4. Imaginary part of the cross-correlation of pol1 and pol2.

These quantities are integrated to the desired time constant (set to 0.516 millisecc for this work) by the GPA Receiver and then written out to the data acquisition system for recording on the main computer system. Typical observation durations used in this experiment were ~ 25 seconds of data.

Offline processing was used for estimation of the mean values (per spectral channel) of the self powers and the cross-correlation amplitude and phase (after proper vector averaging over the duration of the observation). Both raw and normalized values of the cross-correlation amplitude were computed. All values of normalized cross correlations are reported as percentages in this report.

The above back-end system was used to obtain the cross-correlation between the two polarization signals for different kinds of input connections to the samplers in the correlator. For calibrating the set-up, noise source signals of the required properties were injected at the input to the samplers, with the power levels adjusted to be close to the required value of 0 dBm. For studying the polarization properties of the antennas, the baseband output signals were connected to the samplers. Almost all the tests were carried out with AGC off and the antennas were configured appropriately to obtain proper signal levels at the sampler inputs. All experiment were carried out with MCM5 (the MCM for front end control) switched OFF, except one experiment to test the effect of MCM5 on levels of correlated noise in the two polarizations.

In most cases, these experiments were carried out by selecting, in the GAC, the *same* antenna for both polarizations. For a few specific cases, signals from *different* antennas were selected for the two polarizations, in the GAC. We will refer to the first kind of tests as “self-polar” mode tests and the second kind as “cross-polar” mode tests.

The majority of the experiments using actual antenna signals were carried out for the 325 MHz band and only a few in the other bands. *Unless mentioned otherwise specifically, all the experiments and results (for antennas) described below are for the 325 MHz band of the GMRT.* The bulk of the observations were carried out during the period January to April, 2001, with a few early tests dating back to late 2000.

The procedure to configure the GAC and GPA receiver is explained in full detail in Appendix A. Details on how to acquire and analyse the data are given in Appendices B and C.

4 Calibration of the Measurement Tool

Our first step was to calibrate the performance of our measuring tool – the correlator and GPA receiver combination. Specifically, we wanted to quantify the amount of polarization leakage present in this system.

For this, the tests described below were carried out.

4.1 Uncorrelated Noise Test

For measuring the leakage in the correlator + GPA receiver combination, signals from two different (uncorrelated) noise generators were injected as the inputs to the sampler card which would normally receive the two orthogonal polarization signals from one sideband of one antenna. Figure 1 shows the amplitude (normalized and converted to a percentage value) and phase of the cross-correlation between these two signals as a function of frequency channel number, as measured by the GPA receiver. Since one of the noise generators had a bandwidth of only 10 MHz, results for this test are shown only upto channel 150, out of the full 256 channels. The results show that the leakage between orthogonal polarization channels in our back-end system has a mean value of the order of 0.1 %. Most of this is expected to be in the sampler card itself, and our value is consistent with the test measurements carried on the sampler (Shaikh & Roshi, 2000), which yield measured cross coupling of about -27 dB. Further, the phase variation across the channels is random with no signs of any systematic trend or behaviour.

4.2 Correlated Noise Test

The second test to check the performance of the back-end system was to inject fully correlated noise at the inputs of a sampler card and measure the amount of cross-correlation. Figure 2 shows the typical results for this test. The amplitude shows ≈ 100 % correlation and the phase shows a nearly constant value close to zero, with only a very small gradient across the band.

5 Sampler Leakage Tests

The uncorrelated noise source test described above gives a convenient way to characterize any sampler card for the cross-coupling between its two channels. This was also needed for us before measurements with actual antenna signals connected to different samplers could be carried out. Hence we ran these tests on all the 30 pipelines in the current correlator system. The results are summarized in Table 1 as average (over the band) values of the cross-correlation for the uncorrelated noise test. Most sampler chains (except for two) were found to show the expected level of leakage. For the two bad cases (pipelines 4 & 9), the leakage was very high (~ 20 %) and the phase was also constant across the band – see figure 3 for an example. For these two cases, the performance was found to become acceptable after the sampler cards were replaced with spare ones later on. Meanwhile, for all our other tests, we omitted these two pipelines.

6 Checking RF, IF and BB systems

In order to understand the overall polarization properties one needs to understand the electronic chain and estimate the contribution of each block separately. As discussed in Sections 4 & 5, the calibration for the last block – the correlator and GPA receiver – has been done and found healthy. Ideally, the next step would be to inject uncorrelated noise at the baseband and measure the contribution of baseband system for leakage and then work ones way up the chain. However, there are no readily available methods to test these blocks in isolation and hence, we have concentrated on tests related to the front-end electronics section. Here, it is easier to isolate the front-end electronics from the rest of the receiver chain (under software control) and test the latter for polarization leakage. The tests conducted are described below.

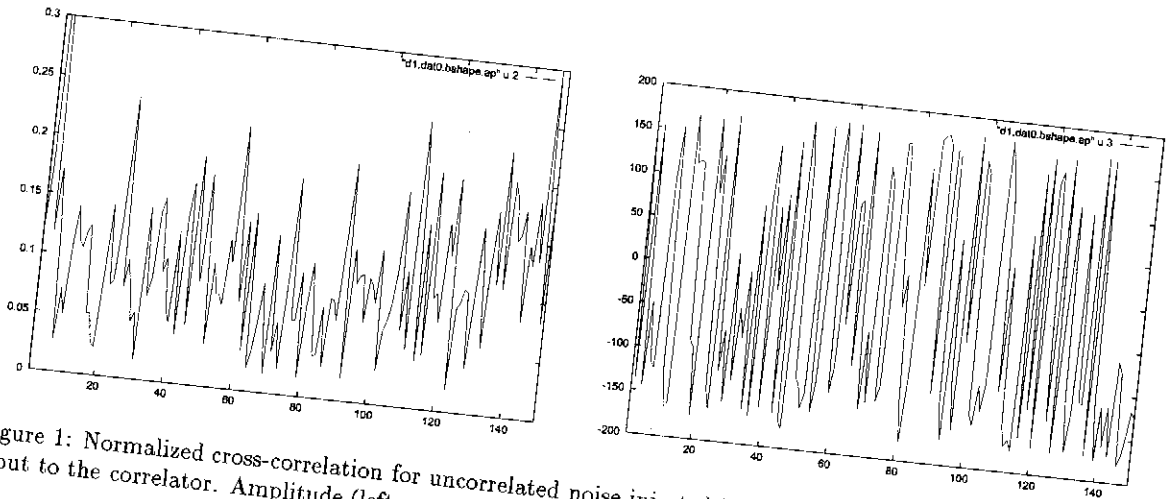


Figure 1: Normalized cross-correlation for uncorrelated noise injected in the 2 polarizations of a sampler at input to the correlator. Amplitude (left panel) in % and phase (right panel) in degrees.

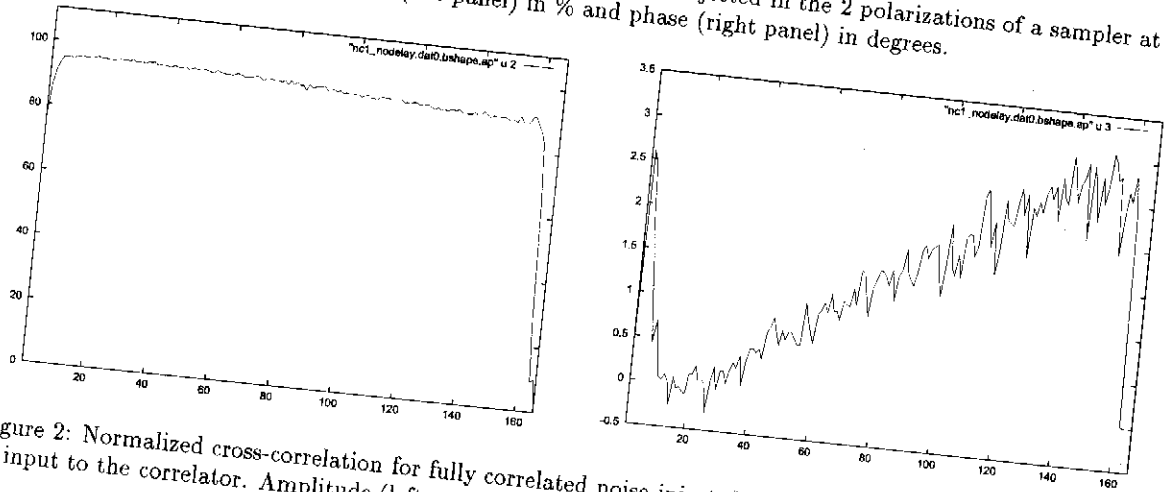


Figure 2: Normalized cross-correlation for fully correlated noise injected in the 2 polarizations of a sampler at input to the correlator. Amplitude (left panel) in % and phase (right panel) in degrees.

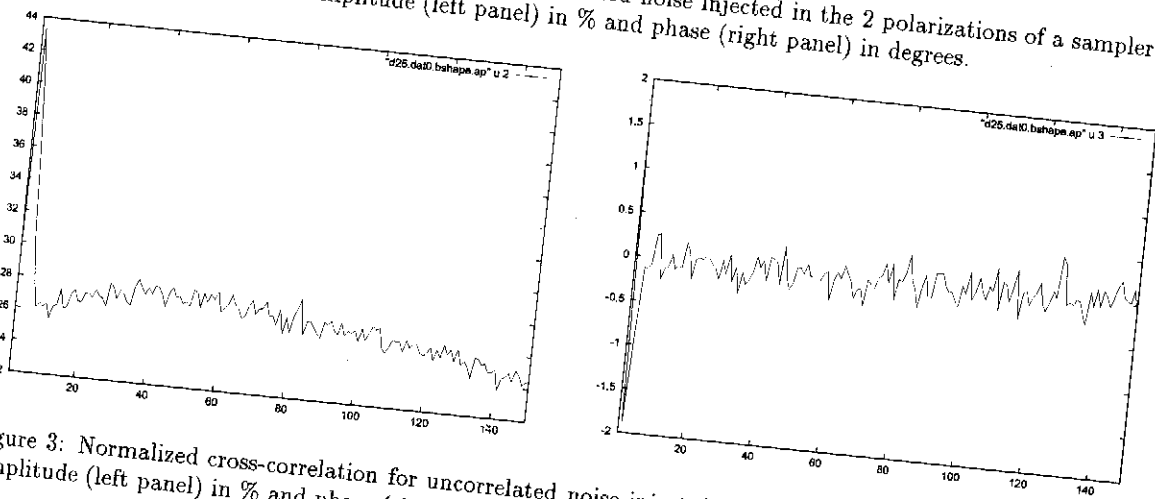


Figure 3: Normalized cross-correlation for uncorrelated noise injected at the input to a bad sampler card. Amplitude (left panel) in % and phase (right panel) in degrees.

Table 1 : Leakage between two channels for all samplers

Samp No.	GAC Dish No.	Leakage
0	21	0.1%
1	22	0.1%
2	23	0.2%
3	24	0.15%
4	25	25%
5	26	0.1%
6	27	0.1%
7	28	0.1%
8	29	0.1%
9	30	22%
10	11	0.1%
11	12	0.1%
12	13	0.1%
13	14	0.1%
14	15	0.1%
15	16	0.1%
16	17	0.1%
17	18	0.1%
18	19	0.1%
19	20	0.1%
20	1	0.1%
21	2	0.1%
22	3	0.1%
23	4	0.1%
24	5	0.1%
25	6	0.1%
26	7	0.1%
27	8	0.1%
28	9	0.1%
29	10	0.1%

6.1 Front End Termination Test

In this experiment, we used the front-end (FE) termination facility to isolate the FE system (up to part of the common box) from the rest of the downstream electronics. Here the receiver noise from the last part of the common box onwards is used as the test signal. After FE termination, the IF attenuations were adjusted to attain the required signal levels at sampler inputs. These experiments were done for two cases – MCM5 in ON and OFF conditions – as we found significant difference in the performance in these two cases. Figure 4 shows the results for these. When MCM5 is OFF, the leakage levels are found to be very similar to the case for the uncorrelated noise source test at sampler input (see section 4), i.e. $\sim 0.1\%$. However, when MCM5 is ON, there are big spikes throughout the band equally spaced at ~ 1 MHz. The peak value of the leakage is 3.7 %, much higher than the mean level when MCM5 is OFF.

This experiment was repeated for almost all antennas and was found to give the same result, with only some small variations in the amplitude of the leakage term.

6.2 RF-OFF Test

In this experiment, instead of using the FE termination command, we used the “RF-OFF” command to isolate the front-end electronics (up to the last stage of the FE box) from the rest of the chain. In this case, we obtained a result similar to the FE termination case when MCM5 is OFF. However, when MCM5 is ON, the spikes in the band are found to be significantly stronger than for the FE termination case, going upto $\sim 20\%$ (see figure 5). Further, even for the channels where the spikes are not there, the leakage term is of the order of 1.0% , which is substantially more than the FE terminated case, where it is $\sim 0.1 - 0.2\%$.

These experiments clearly show that, under MCM5 off conditions, there is no leakage in the system, after the common box of the FE system. Hence there is no need to individually check the ABR, fiber optic and baseband units for cross-coupling.

6.3 Phase response

The phase response for the RF-OFF test with MCM5 ON (see figure 6) shows a systematic behaviour in the form of a linear gradient across the entire band. A similar result is obtained for the FE terminated case. This can be explained if there is an effective delay between the two polarization paths as they traverse the analog electronics chain before reaching the correlator. Alternatively, it is possible that the correlated signal that is seen in the two polarizations couples in with a relative delay between the two polarizations, but this is rather unlikely (see section 7.1 for more on this).

6.4 Conclusions

From the two experiments described above we conclude the following:

1. When MCM5 is OFF, it appears that the electronics chain from common box input down to the baseband output does not have any significant polarization leakage nor any correlated signal pick-up. This conclusion needs to be verified with stricter tests, as it gives a “clean chit” to a large part of the chain : common box, ABR, fiber optic and baseband systems.
2. When MCM5 is ON, it appears that there is source of correlated signal pick-up in the two orthogonal polarization signal paths, with the correlated signal having a periodic 1 MHz comb nature. The typical strength of this pick-up is ~ 5 percent of the effective receiver noise for the FE terminated case (and ~ 20 percent for the RF-OFF case). Now, such a 1 MHz comb signal is seen in the total power outputs of most of the antennas, during normal observations (predominantly in the 150 and 235 MHz bands), when MCM5 is left ON. This, so far, has been believed to be due to *radiative* pick-up, by the feeds, of some signal generated (and transmitted out of the FE box) by the MCM5 electronics. However, these results (especially for the case of RF-OFF) indicate that this pick-up *may be electrically coupled inside the FE electronics*. If confirmed, this would require a close look at the design and layout of the electronics in the FE system, as the possibility of other unwanted signals coupling through this same path is quite likely. The fact that there is an increase in the strength of the normalized cross-correlated signal, from the FE terminated to the RF-OFF case, should throw some light on the matter.

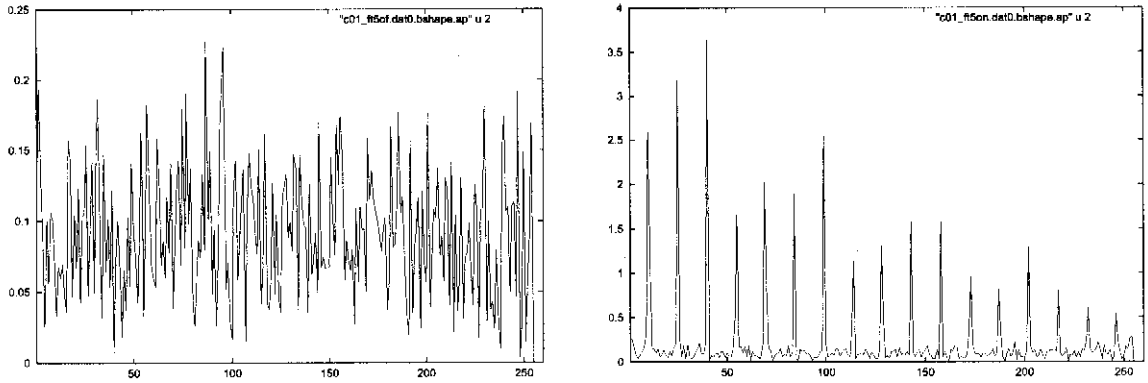


Figure 4: Normalized cross-correlation (amplitude in %) for Front End terminated : MCM5 OFF (left panel) and MCM5 ON (right panel).

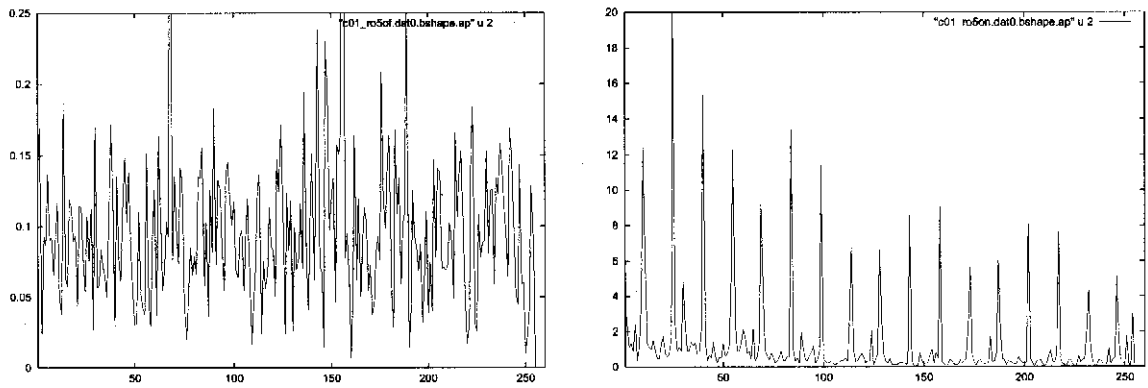


Figure 5: Normalized cross-correlation (amplitude in %) for RF-OFF case : MCM5 OFF (left panel) and MCM5 ON (right panel).

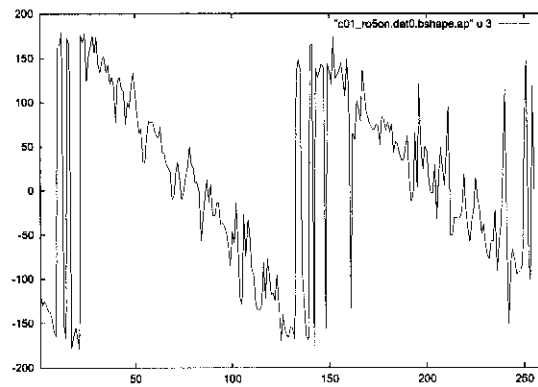


Figure 6: Phase for the normalized cross-correlation in right panel of figure 5 – MCM5 ON case.

7 Antenna Tests No. 1 (Self-Polar Mode)

To check the polarization cross-coupling of the complete antenna, we need to test with signals from celestial sources coming in through the feed system and passing through the full electronics chain. In this section, we describe some of these tests, carried out in the “self-polar” mode. In this mode, the two polarizations of the *same* antenna are selected in the GAC and cross-multiplied in the GPA receiver. The experiment was done for antennas pointing ON-source and OFF-source, using standard calibrator sources. It was repeated for different conditions to test various ideas. Several antennas were tested in this mode.

7.1 Basic Results

Following the results for different models described in equations 10 to 12, for an unpolarized continuum calibrator source, we expect to see some finite value for the amplitude of the cross-correlation between the two polarizations, if there is some leakage between the two polarization paths in the dish, feed and front-end electronics. For the case of model 1 (described by equation 10), the value should be significantly more than that for a nearby “OFF-source” position and should increase with increasing source strength, saturating to a constant value for source temperature much larger than the receiver noise temperature.

However, what we find from our experiments is quite different. In most cases, the normalized cross-correlation actually *reduces* when going from OFF-source to ON-source (see figures 7 and 8 for examples). Further, the reduction is found to be *more* for *stronger* sources, quite opposite of what is expected (see for example, figure 9 which shows the correlation for C04 on different sources : 3C218, 3C286, 3C295 & 3C353). Correspondingly, the raw (or unnormalized) cross-correlations maintain a roughly constant level irrespective of OFF- or ON-source position of the antennas, and also for ON-source positions for different sources (for the cases where the antenna gain is not changed to compensate for the power level changes) – see figure 10 for a typical example of this. Further, it is also seen that the band-averaged normalized cross-correlation for off-source observations reduces for regions of the sky where the total system noise temperature is higher (due to increase in background temperature) – for example, compare the two OFF-source curves in figure 8, where OFF-source for 3C295 is in a colder part of the sky than that for 3C353.

The above results can be explained if the cause for the cross-correlation is not due to genuine cross-coupling between the antenna signals from the two orthogonal polarizations, but due to a source of noise pick-up that is correlated between the two polarizations (as described by model 3 – equation 12 in section 2). Note that though an alternative like model 2 (equation 11 in section 2) can explain some of the above features, it can not explain all the data; hence model 3 is the preferred model here. A correlated noise source of the order of 5-8 % of the system noise temperature is needed to explain these results.

The phase of the cross-correlation measured between the two polarizations typically shows a significant phase ramp for most of the antennas. Figure 11 shows an example for the case of C01 pointing to blank sky. The slope corresponds to about a 4 clock cycle (~ 130 nanosec) effective delay between the two signals being correlated. Note that this slope is very similar to that seen in figure 6 (for the “RF-OFF” test involving the same antenna), indicating that the same underlying cause is operative in both conditions. The ramps seen for most antennas are in the range of 3 to 5 clock cycles (~ 100 to 160 nanosec) of delay. Further, the phase ramp for a given antenna maintains its basic slope for all the different kinds of tests involving different sources and reconfigurations in the front-end electronics. All this strongly supports the view that the delay seen is due to the difference between the signal path for the two polarization channels, accumulated somewhere in the IF chain. One likely cause is differential propagation delay in the SAW filters used in the IF system.

7.2 W02 : A Special Case

An extreme case of the abnormal cross-correlation between the two polarizations was seen for W02, where it was found to be substantially higher than for most other antennas (at 325 MHz) : upto 20 % in some parts of the band (see figure 12). Once again, it shows some tendency to reduce with increasing source strength. This result may have some correlation with the fact that, during this period, the normalized fringe amplitude on baselines involving W02 was always found to be less than that for other baselines in the correlator.

7.3 Effect of Ground Reflections ?

In order to check if there was any common source of radiation outside the dish surface (e.g. spillover + spurious ground reflections) seen by both polarizations of an antenna, the tests were repeated with *feeds* pointing to the sky (instead of illuminating the dish). The results (see figure 13 for a typical example) show that there is still a cross-correlation of the level of $\sim 5\%$ that is present (though the shape across the band is somewhat different). This tends to support the presence of a common source of noise pick-up in the electronics.

7.4 Effect of MCM5

Some of the tests described above in this section were also carried out with MCM5 in the ON condition. In most cases, the cross-correlation does *not* show the spikes seen in the case of the front-end terminated and RF-OFF tests. This could be explained if the spurious correlated pick-up producing the spikes occurs *after* the LNA stage, as the correlated noise power then will be a very small fraction of the effective receiver noise, which is dominated by the LNA.

7.5 Conclusion

From the self-polar mode tests described in this section, we are led to the following conclusion :

There is very likely a common source of noise that is leaking into both polarization channels in the front-end electronics system of the 325 MHz band of the GMRT. The typical value of this noise is $\sim 5-10\%$ of the system noise, with a worst case of about 20 %.

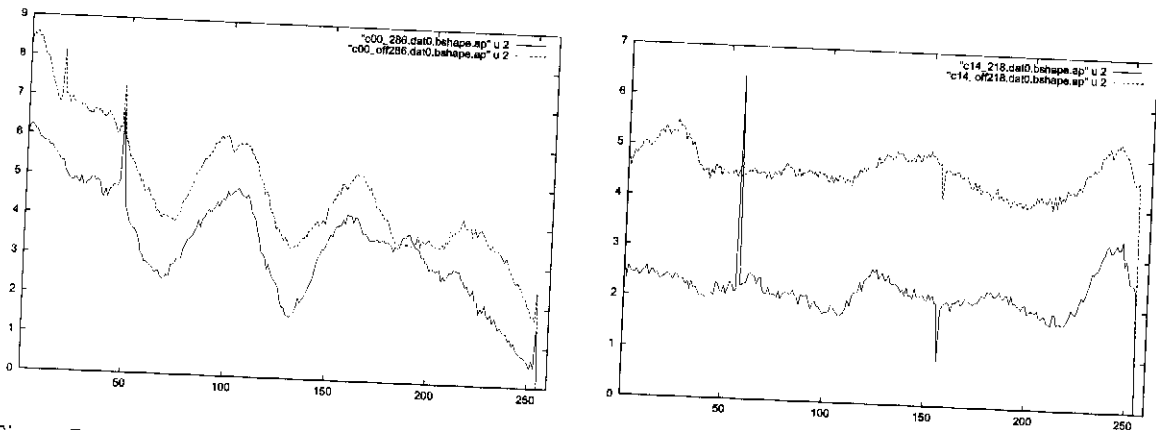


Figure 7: Normalized cross-correlation (amplitude in %) for C00 -- ON & OFF 3C286 (left panel, solid & dashed curves, respectively) & for C14 -- ON & OFF 3C218 (right panel, solid & dashed curves, respectively).

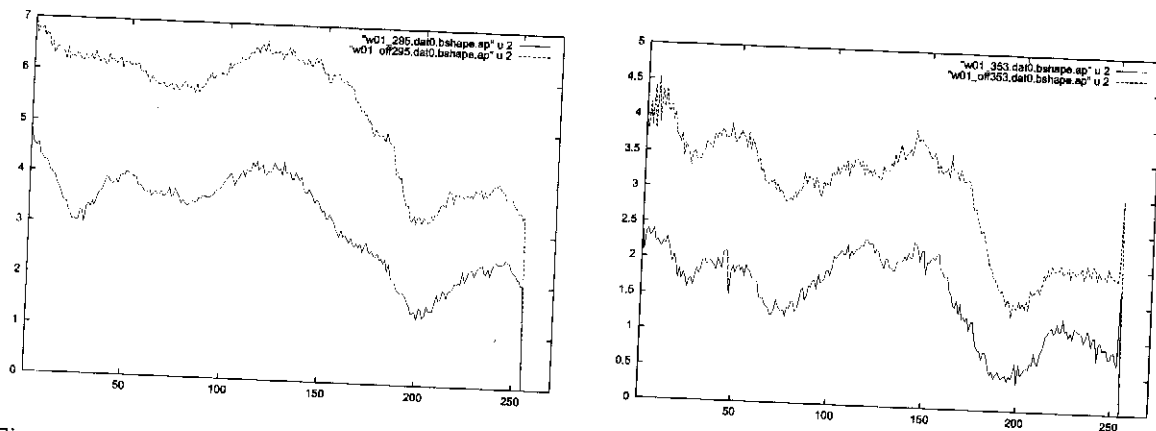


Figure 8: Normalized cross-correlation (amplitude in %) for W01 -- ON & OFF 3C295 (left panel, solid and dashed curves, respectively) and for W01 -- ON & OFF 3C353 (right panel, solid and dashed curves, respectively).

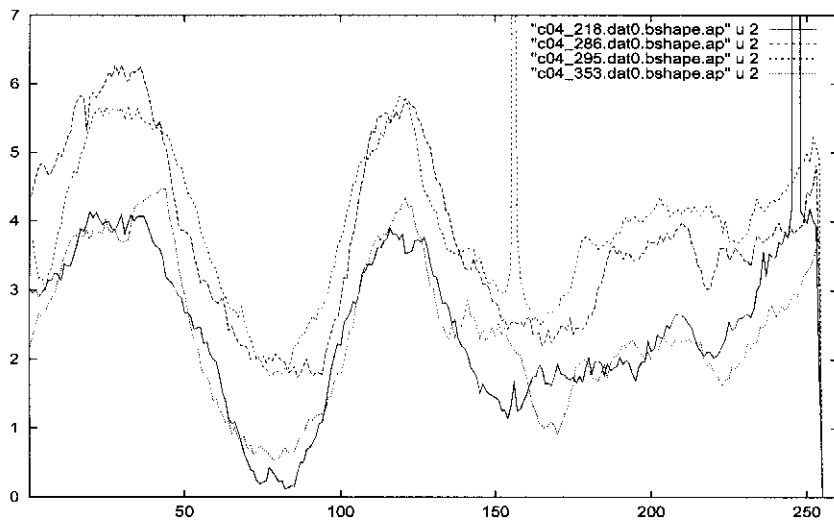


Figure 9: Normalized cross-correlation for C04 for ON-source on 3C286 (27 Jy), 3C295 (61 Jy), 3C353 (148 Jy) & 3C218 (163 Jy).

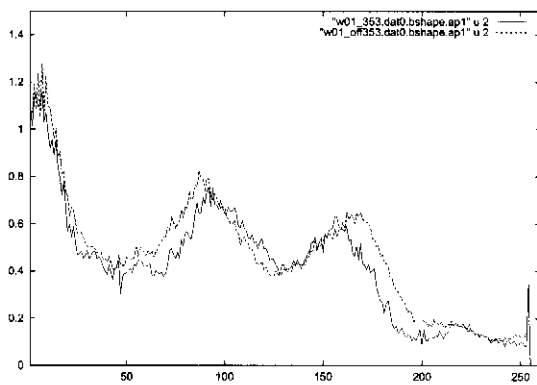


Figure 10: Unnormalized cross-correlation for W01 for ON & OFF 3C353 (solid and dashed curves, respectively).

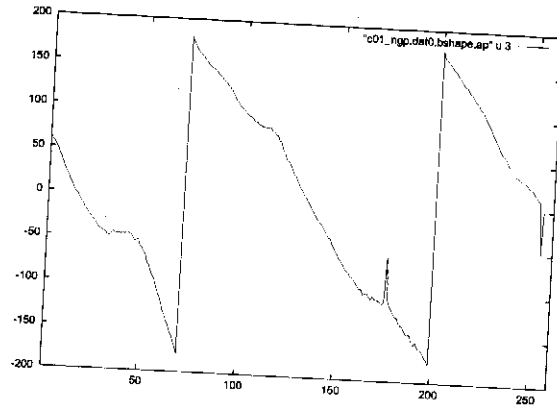


Figure 11: Phase for the normalized cross-correlation for C01 on blank sky.

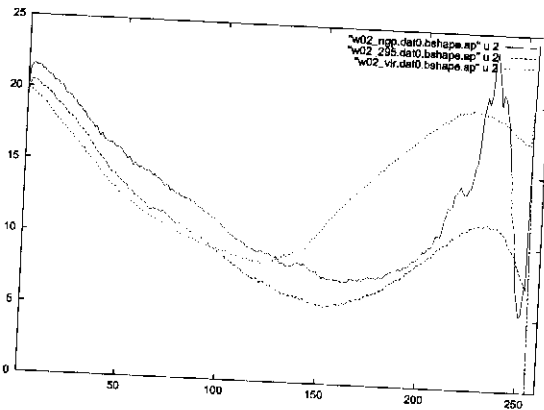


Figure 12: Normalized cross-correlation (amplitude in %) for W02 on blank sky, 3C295 & VirgoA.

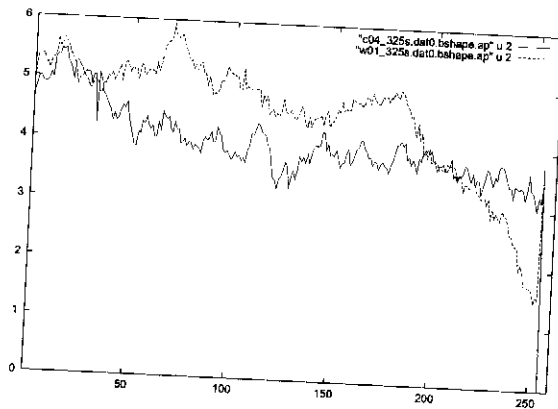


Figure 13: Normalized cross correlation (amplitude in %) for C04 & W01 with feed pointing to sky

8 Antenna Tests No. 2 (Cross-Polar Mode)

As the previous tests give strong evidence for the presence of a common source of noise in the two polarization channels for the GMRT antennas, we did some “cross-polar” mode tests to try and resolve the issue. In this mode, polarizations of two *different* antennas are selected in the GAC and their cross-correlation is measured by the GPA receiver. Further, by using the RF swap facility in the front-end electronics, same or different polarizations of the two antennas can be correlated. In the former case, it is very much like a visibility measurement for the corresponding baseline, while the latter will be sensitive to the leakage between the two polarizations with the benefit of not responding to any common pick-up which may be present in each antenna individually, as long as this pick-up is uncorrelated between different antennas. Both antennas involved were pointed to the same source and full “fstop” correction was implemented in the correlator. The following tests were done in this mode.

8.1 Off Source (Blank sky) Tests

In this experiment, the visibility and leakage cross-correlations were measured when the antennas were tracking OFF-source from the calibrator. The leakage measurements for almost all pairs of antennas show very low levels of cross correlation (~ 0.1 to 0.2 %) with random phase – quite similar the levels obtained from uncorrelated noise source tests done during the calibration of the back-end (section 4). Figure 14 shows the typical results. The visibility measurements for OFF-source observations (see figure 15 for an example) also show results quite similar to the leakage measurements (except for what may be a minor increase in the cross-correlation level). This is what one would expect for the blank sky case as there should be no correlated signal present between either of the two polarizations from two different antennas.

8.2 On Source Tests

In this experiment, the visibility and leakage cross-correlations were measured when the antennas were tracking ON-source for a nominally unpolarized calibrator source. Sample results are given in figures 16 and 17, which show visibility and leakage terms for a given antenna pair, for two different sources. The visibility amplitudes are as expected and change in accordance with the expected values of the source and system temperatures and the baseline value. The leakage terms are much smaller than the corresponding terms obtained from self-polar mode tests involving either of the two antennas. Equally importantly, they scale in accordance with the strength of the calibrator source, unlike the self-polar measurements. This tells us that we are now seeing the *real* polarization cross-coupling in the antennas, rather than the effect of some common pick-up in the two polarization channels of the antennas.

A first order estimate of the polarization cross-coupling can be obtained from the ratio of the leakage cross-correlation to the visibility cross-correlation. For a simple model of the cross-coupling being identical in all antennas and assuming all gain terms are properly taken care of, this ratio is $\sim 2 \times \text{Re}[\epsilon_{RL}]$. Estimates from the data (e.g. figure 18) yield values ~ 1.5 to 2.5 % for the cross-coupling coefficient. One exception was C14, for which results with respect to all antennas consistently showed slightly higher values (~ 3 to 5 %). The above numbers were found to be consistent across different sources used for the tests.

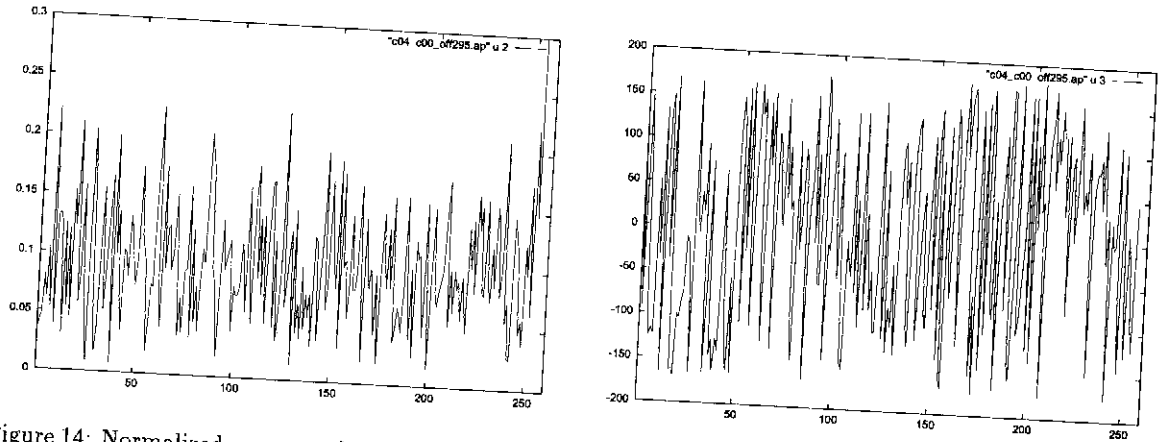


Figure 14: Normalized cross-correlation (LEAKAGE mode) for C04-C00 OFF-source from 3C295. Amplitude (left panel) in % and phase (right panel) in degrees.

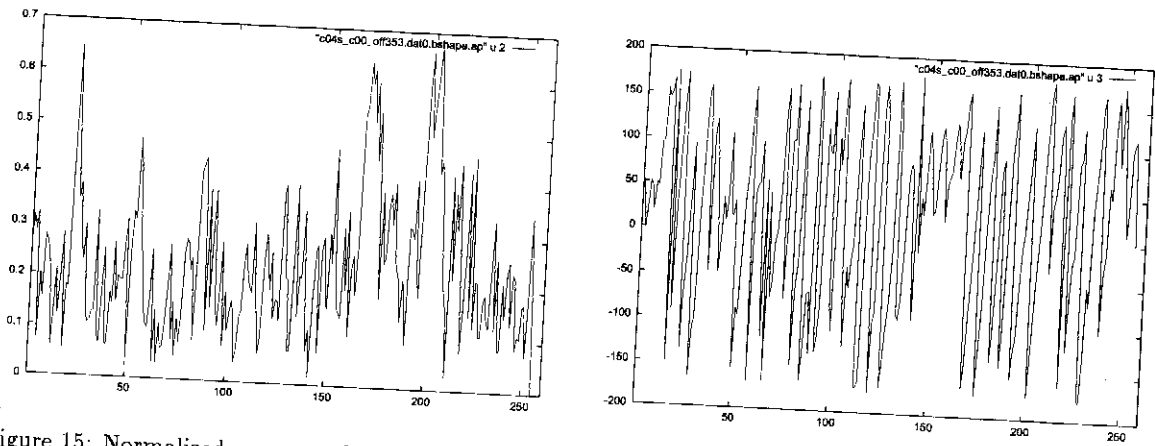


Figure 15: Normalized cross-correlation (VISIBILITY mode) for C04-C00 OFF-source from 3C353. Amplitude (left panel) in % and phase (right panel) in degrees.

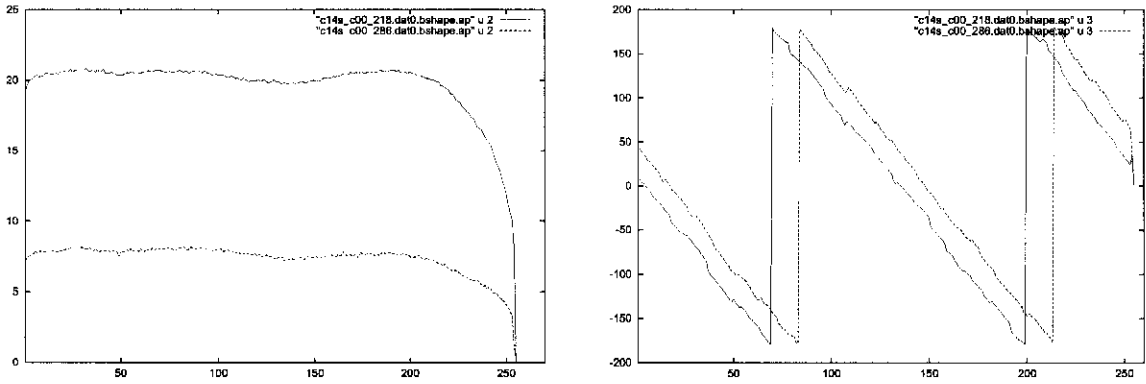


Figure 16: Normalized cross-correlation (VISIBILITY mode) for C14-C00, ON-source for 3C295 & 3C353. Amplitudes (left panel) in % and phases (right panel) in degrees.

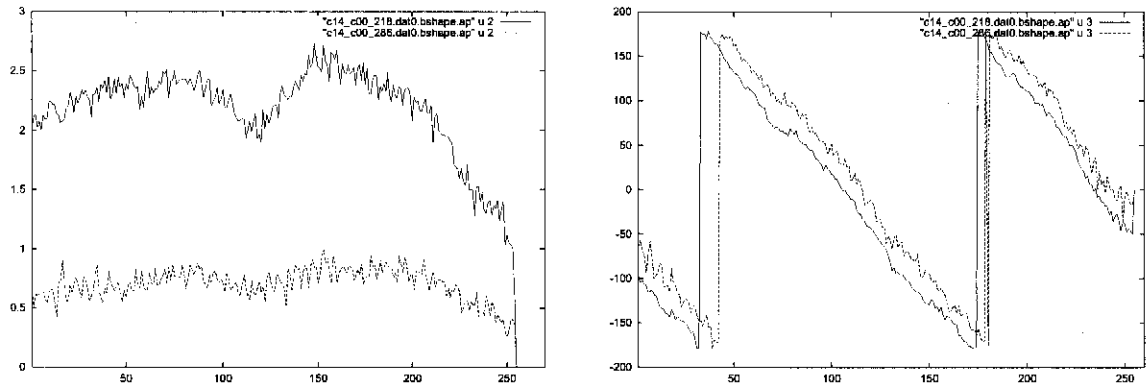


Figure 17: Normalized cross-correlation (LEAKAGE mode) for C14-C00, ON-source for 3C295 & 3C353. Amplitudes (left panel) in % and phases (right panel) in degrees.

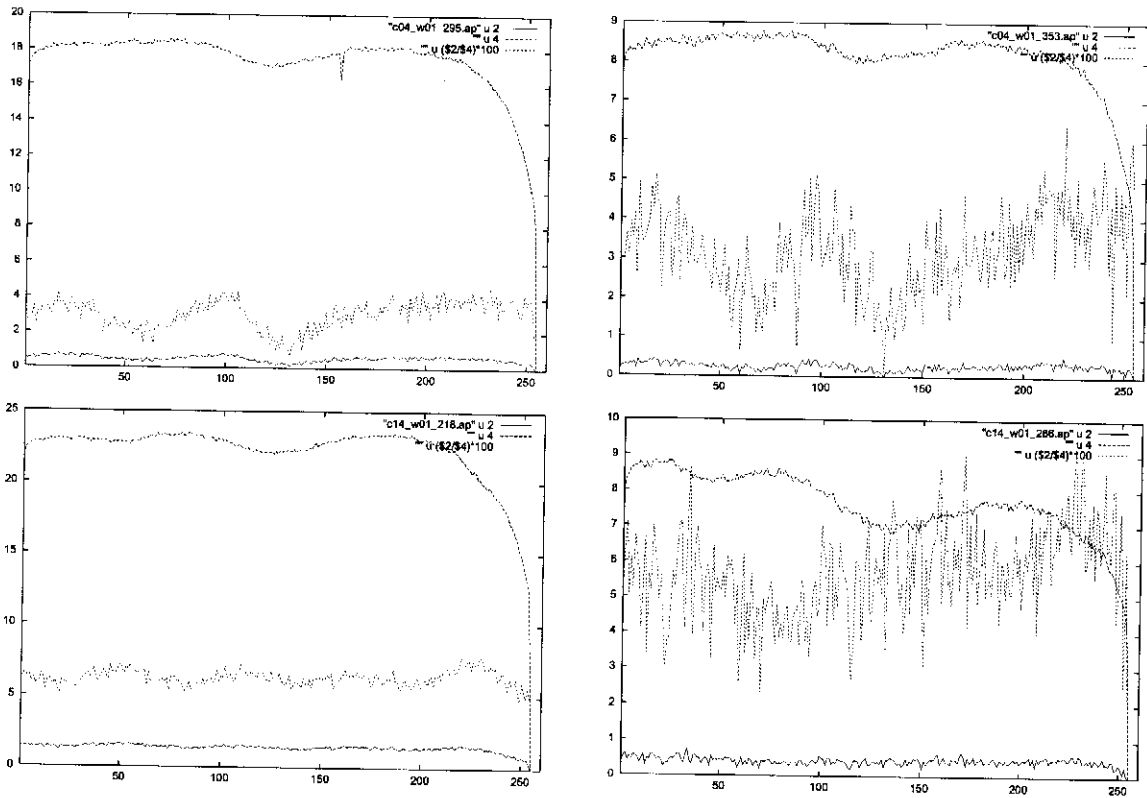


Figure 18: Normalized cross-correlations (amplitude in %) for leakage mode (solid lines) and visibility mode (dashed lines), along with their ratio multiplied by 100 (dotted lines) for different baselines and different sources.

9 Results for other frequency bands

Though most of our work concentrated on experiments in the 325 MHz band, some tests were also done for the 150, 235, 610 and 1400 bands. Of these, the most detailed results are available for 610 MHz band. For antennas at this frequency, the self-polar mode tests also show evidence for correlated noise pick-up in the two polarizations, as in the 325 MHz case (see figure 19 for a sample of the results). However, one additional feature at this frequency is that there are large variations in the level of the normalised cross-correlation across the band. Usually, there are 3 to 4 wide ripples across the band (e.g. C08, C09 and E06 in figure 19). For some antennas, one of these ripples peaks at a very large value (with almost one order of magnitude increase for the worst case) at some part of the band (e.g. C02, C03 and C10 in figure 19). At first sight this implies a significantly larger value of the correlated noise at selected parts in the band.

Results from the cross-polar mode tests at 610 MHz also show interesting features. Figure 20 shows the visibility and leakage cross-correlations for three antennas of figure 19, against C09. Both C02 and C10 show large drops in the visibility measurement around exactly those points in the band where the normalized cross-correlations in figure 19 have their highest values. Clearly there is a connection between these two effects. The most likely explanation is that the correlated noise pick-up seen in figure 19 is strong enough to significantly increase the effective system noise temperature at some points in the band, leading to a fall

in the normalized visibility at those points. Note that the visibility fluctuations across the band for several antennas at 610 MHz (and, equivalently, total power sensitivity variations across the band) have been known for a long time now. These have been ascribed to a variation in the strength of the source signal picked up by the antenna as a function of frequency in the band (thought to be due to problems with the feed design at 610 MHz), rather than to variations in the effective noise temperature in different parts of the band. These results should provide sufficient reason to examine this postulate afresh.

For the specific case of C02 at 610 MHz, from the visibility measurements in figure 20, the *extra* contribution to system noise temperature of C02 required to explain the maximum dip near channel 50 (assuming normal receiver noise temperature for C09 and identical degrees K/Jy for the two antennas) is about 120° K – somewhat more than the nominal total receiver noise temperature. This is also consistent with the \sim factor of 2 loss of effective sensitivity seen for this antenna around this channel in total power sensitivity measurements using the incoherent array mode pulsar receiver. However, in order to explain the peak of the curve for this antenna in figure 19 using equation 12, a value of T_c of about 50° K is required. Thus there is some quantitative inconsistency between these two requirements. This can be resolved if the common noise source couples into the two polarizations of this antenna with *different amplitudes*. An amplitude imbalance of 0.2:1 is needed to explain the results of figures 19 and 20 for this antenna.

From the ratios of the leakage and visibility mode cross-correlations in figure 20, a rough estimate of the genuine cross-coupling can be obtained. The typical numbers are a factor of 2 or more higher than those for the 325 MHz data, being more like $\sim 5\%$ for most antennas at 610 MHz.

From our sparse tests at other wave-bands, we find that there is evidence for correlated signal pick-up in all the GMRT wave-bands. Results at 235 MHz also tend to show some large relative fluctuations across the band, similar in nature to the 610 results.

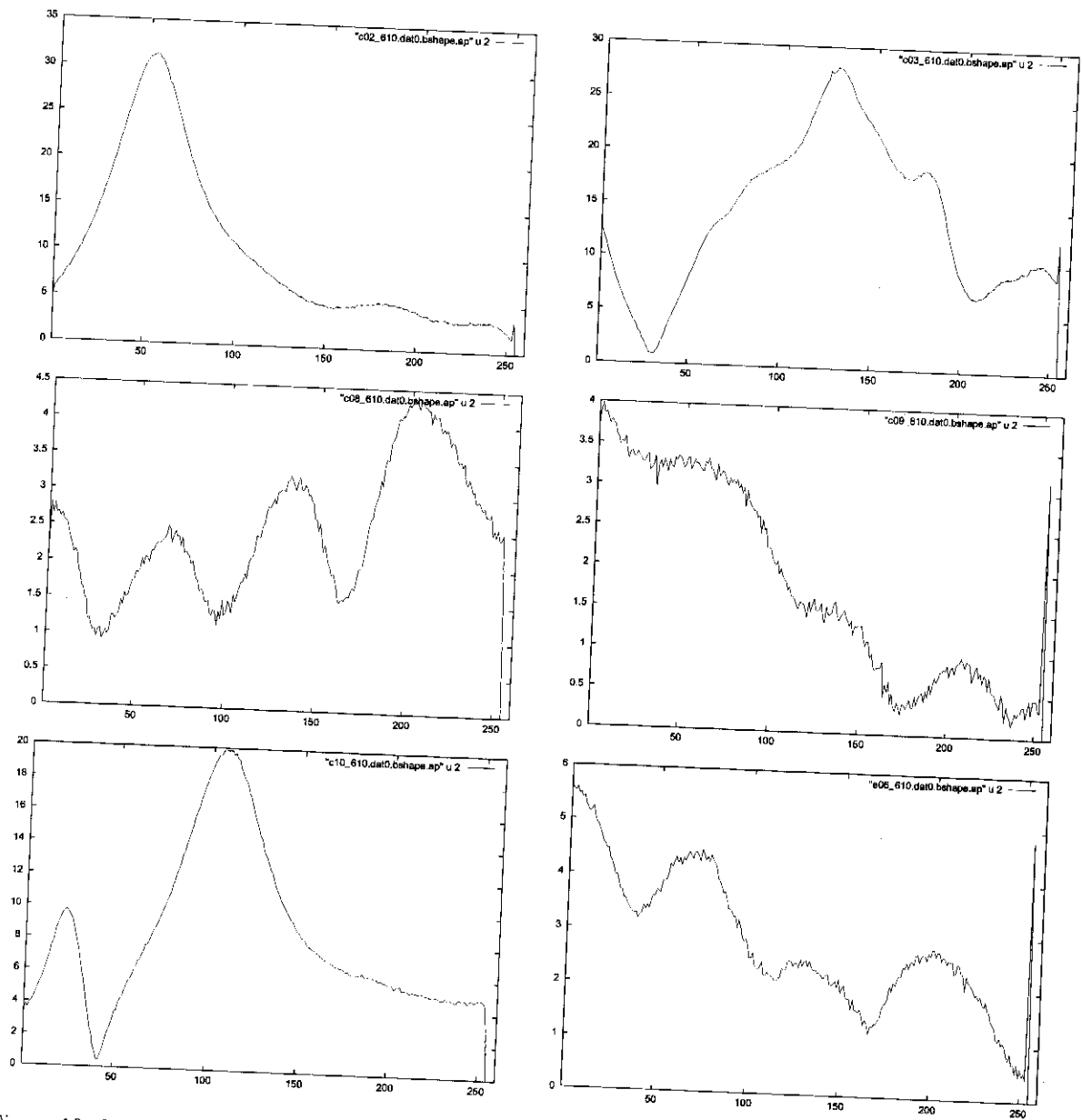


Figure 19: Normalized cross-correlations (amplitude in %) for 3C147 ON-source for C02, C03, C08, C09, C10 & E06 - all at 610 MHz.

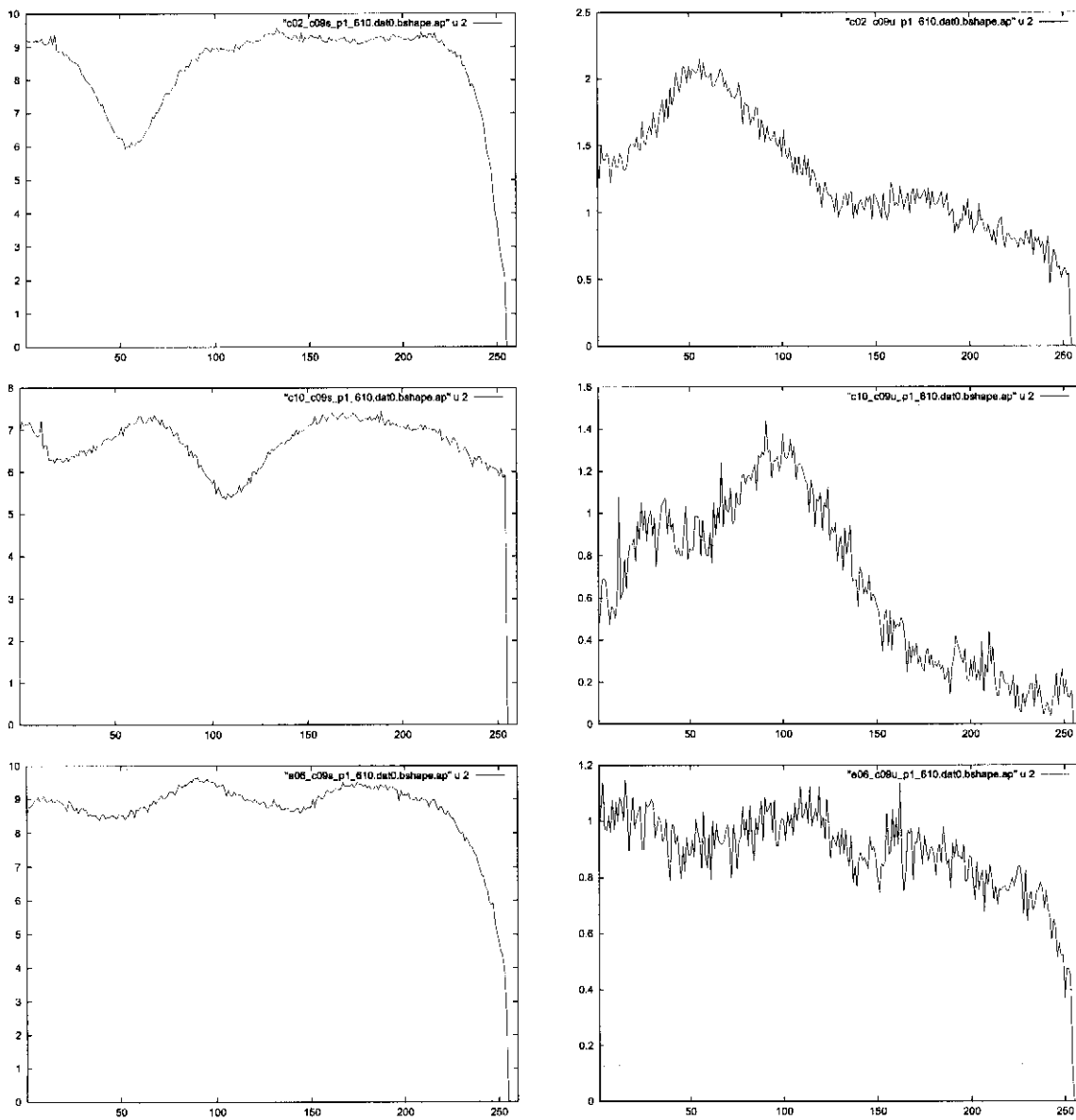


Figure 20: Normalized cross-correlations (amplitude in %) for VISIBILITY mode (left panels) and LEAKAGE mode (right panels) with 3C147 ON-source; for C02-C09 (top), C10-C09 (middle) & E06-C09 (bottom) – all at 610 MHz.

10 Conclusions and Future Prospects

The main conclusions from this work can be summarized as follows :

1. When MCM5 is OFF, it appears that the electronics chain from common box input down to the baseband output does not have any significant polarization leakage nor any correlated signal pick-up. This conclusion needs to be verified with stricter tests, as it gives a "clean chit" to a large part of the chain - common box, ABR, fiber optic and baseband systems.
2. When MCM5 is ON, it appears that there is a source of correlated signal pick-up in the two orthogonal polarization signal paths. This correlated signal consists of a stronger component that has a periodic 1 MHz comb nature, and a weaker broadband component. It appears that this MCM5 generated noise is *electrically coupled* to the RF signal path, rather than *radiatively coupled* via the feed. This problem deserves immediate attention, to find and eliminate the cause of this electrical coupling, as other sources of noise in the FE system could also find themselves coupling through this path.
3. In addition to the MCM5 generated noise, the tests strongly support the presence of *another* source of broadband noise that leaks into both polarization channels of the antennas. This source of noise, which has a typical amplitude ~ 5 to 8% of the system noise at 325 MHz (with a worst case value of $\sim 20\%$ for one antenna), is most likely located somewhere *ahead* of the common box in the electronics chain. It appears to be present at all frequency bands (with differing strengths), indicating a fairly broad-band nature of the noise source. For some wave-bands (like 610 MHz, and to a lesser extent, 235 MHz), for several antennas, its strength varies significantly across the band. At 610 MHz, strong increases are very well correlated with decreased SNR from the antenna at that part of the band - this extra source of noise may well be the cause for the by now well known feature of effective loss of sensitivity for many antennas at different points in the 610 MHz band.

One experiment that will help to determine if the source of this noise is truly in the FE box or not, is to physically terminate the inputs to the FE box (i.e. the signals coming from the feed dipoles) and repeat the self-polar mode tests. Again, it is of some importance to track down and locate the source of this correlated signal, as it will significantly corrupt all attempts at polarization calibration of the antennas.

4. Using the cross-polar mode of tests, we find that a ball park value for the real polarization cross-coupling at 325 MHz is ~ 1.5 to 3% , and more like $\sim 5\%$ for 610 MHz. More rigorous tests with polarized sources will be needed to get down to the exact values of the amplitudes and phases of the cross-coupling parameters. In this context, we now have a well tested and working set-up that can be used for polarization calibration measurements, on polarized continuum calibration sources as well as on pulsars.

11 References

1. Gupta & Upreti, NCRA Internal Technical Report 090210 (1991).
2. Conway & Kronberg, MNRAS, 142, 11 (1969).
3. Sirothia, M.Sc. thesis, Pune University (2001).
4. Shaikh & Roshi, NCRA Internal Technical Report (2000).

A Configuring GAC and GPA-receiver

A.1 GAC configuration

The GAC (GMRT Array Combiner) which has the capability to add the signal from any number of selected antennas (independently for each of the two polarizations) in either incoherent or coherent array mode, is most conveniently configured from within the main pulsar receiver control software environment (the “pulsar console”). Here, one can conveniently click and choose the desired polarizations of the selected antennas, independently for the incoherent and phased array modes.

A.2 GPA receiver Configuration

Configuring GPA receiver involves the machine called DASPC. Log in on DASPC as “das” and run the program

```
/home1/das/das/sirothia/fft/fc_pkt_lin.
```

First line of the output of this program should be

```
Default Link, 0 already open,
```

which indicates that, device driver is loaded and installed properly while booting the machine. This program asks for options. Follow the options listed below :

97 To reset control cards.

0 To download an executable file.

It will prompt for the file name to download. Give a file name **stoke_dsp.exe**

If during downloading it gives an error, then there is a hardware problem that needs to be referred to the engineers for fixing.

1 To execute the downloaded file.

99 To exit out of the program.

After successful execution of this program run the program

```
/home1/das/das/sirothia/fft/configfft
```

Again, it should run through without any error for proper continuation.

B Data acquisition

This involves two machines called CORRPC and DUAL2. Log in on these two machines as “das”. Every acquisition is initiated by the the program

```
/usr/home/das/das/appli/stock/run
```

on CORRPC. After starting this, start the acquisition program on DUAL2 with the command

```
devcat 10000 1 | rsh mithun -l das "cat > raw_data_filename" 1
```

Watch the output of these two programs to see if there is any error or failure during data acquisition :

The first program *run* should print the message

```
Successfully booted node # card_id
```

for card id 0 through 3.

Output of the *devcat* has much information to be checked before going on to the analysis of the data :

¹Make sure the directory where the file will be written (in mithun) has a write permission for das

1. It should show interrupt count = 10000
2. It should show interrupt overruns = 0
3. It should show dma incomplets = 0
4. It should show data overruns = 0
5. It should show data underruns = 0

C Data Analysis

For analyzing this data user can use the pulsar software available on the machine MITHUN.

The GPA receiver while writing the data, writes the marker in beginning as well as in data at equal interval. To make sure GPA receiver has written the data properly, check whether the raw data file has the marker in it properly placed. At the beginning of every raw data file there are 8192 byte of marker and 8192 nd byte is the last marker and it always has to be *fdfc*. In some case, while writing to file, two extra words (4 byte) gets added to file in the beginning. This can be seen by using the command² as below

```
od -xv -Ad raw_data_file | more
```

Using this command check out if there is proper misplacement. After having checked for the marker shift, removes the marker using the command

```
dd if=infile of=outfile bs=81983 skip=1
```

Use this output raw data file for further analysis with the program as below.

```
psr_dsp_online_mpol.tu file_name 4 1 4 .2 0 0
```

which needs the *psr_online.in* file⁴, with proper entries in it.

This program shows the four output parameter of the GPA receiver, and at the end, it write a file named filename.bshape which contains the various bandshapes, viz. total power in both polarization, and *Real* and *Imaginary* term of cross-correlation. To convert *Real & Imaginary* form to *Amplitude* of the cross-correlation, use the program

```
ri2ap filename.bshape
```

which will produce a filename named, filename.bshape.ap, which in turn will contain *Amplitude* and *Phase* bandshape as a function of spectral channels.

²In later version program will do it automatically.

³8198 instead of 8192 because, polarimeter, by defaults, adds three words (6 bytes) after the marker end, (which will corrected in hardware in later version). In case, the marker is shifted by two words, like *fdfc* is not the 8192 nd byte and is 8196 th byte, use *bs=8202*, which is block size and which is skipped by 1 in output raw data file

⁴File can be found in */d1/systest/ygupta/bsap*